Computational Modeling for Non-equilibrium Shock Tube Flows

Khalil Bensassi, Aaron M. Brandis and Brett A. Cruden
AMA, Inc. at NASA Ames Research Center

Corresponding author: khalil.bensassi@nasa.gov

Abstract Time accurate simulation of non-equilibrium flows inside shock tube facilities presents several challenges from both physical and mathematical aspects. Furthermore, the drastic computational cost makes it non-practical to support real-time experimental test campaign. In this work, we explore other methods for modeling the shock tube problem with the main focus on the post-shock region and the absolute radiation emanating from it. The proposed alternative approach is several orders of magnitude less computationally expansive while still accurate enough with regards to the quantities of interest. Excellent agreement is found with the well-established stagnation-line approach. Comparison with the time-accurate simulation shows good agreement close to the peak values and disagreement of the temperatures relaxation and radiance profiles toward equilibrium, due to shock speed unsteadiness.

1 Introduction

Shock-tube experiments continue to play a primordial role in space mission design. In particular, they are used for the prediction of the spacecraft's radiative heating during Earth re-entry from either a lunar or Mars return mission. For this type of mission, where entry velocity ranges from 10 to 15 km/s, shock layer radiation will constitute 30 to 50% of the total heat flux to the vehicle surface in the peak heating region of the entry trajectory. Shock tube facilities have the capability to generate shock-heated air at velocities and pressures representative of these return trajectories. Spatially and spectrally resolved intensity profiles behind the unsteady shock are obtained from radiation measurement. Thus, details of the post-shock gas state for both equilibrium and non-equilibrium regions are obtained. These data are not only used for assessing the aerothermal loads on the spacecraft but also constitute the holy grail for the computational modeling tribe: benchmark data against which modeling and simulation tools can be validated. In order to achieve this, computational codes need to be able to replicate the flow in such facilities.

Nowadays, computational fluid dynamics is a major tool to study and predict real flight data over the whole (re)-entry trajectory of the space vehicle and are also used, at a much lower scale, to support wind tunnel data analysis. Although, critical for the validation of the physical models, there have only been a limited number of attempts by various authors [1, 2, 3] to model the shock tube experiment in detail. This redoubtable task presents several computational challenges which involve a large number of different physical processes: the heating process in the driver, diaphragm rupture, turbulent mixing of the hot jet of the driver gas and the cold driven gas and radiative losses, to name a few. Some of these processes are not well understood and/or are very complex. Unfortunately, another layer of difficulty is added by the numerical aspect of the problem. The large disparity between the space scale, which is of the order of many meters, and the time scale, which is of the order of nanoseconds makes the problem very stiff. This stiffness is increased by the chemical and kinetics source terms governing the non-equilibrium processes. At the furthermost end, the computational cost is colossal.

In order to overcome the prohibitive computational requirements, and enable support of experimental tests campaign, one need to resort to a reduced model of the problem. These models are computationally less expensive by several orders of magnitude, but still encapsulate the key physical components that offer the potential for a sufficient level of accuracy. One way to achieve this in our case is by reducing the large disparity between space and time scales. Reducing the space scale means investigating only the crucial part of the facility with regards to our quantity of interest. In a context of shock tube problem, where radiative heating is the main concern, one can restrict our numerical investigation to the post-shock region. The time scale reduction can also provide some drastic computational cost reduction, but does come with several assumptions and simplifications. One prominent simplification is that the time dependency is not sought, and steady state solution may be sufficient to achieve the minimum level of accuracy required for our quantity of interest. A posteriori justification of this assumption remains vital.

In this work, we assess two reduced models for the shock tube problem. Both models are multidimensional and we believe they are able to accurately predict the post-shock region using the test section shock speed as the main input. The first model is a flow over a cylinder, and the region of interest is the post-shock region along the stagnation line. We reference this method as the "stagnation-line approach". The radius of the cylinder is taken large enough (3 to 5 m), so we avoid the influence of the wall curvature on the post-shock conditions. The second model is a flow in a 0.30 m tube, it is 25x shorter than the complete shock tube. The inlet flow velocity is equal to the test section shock speed, and the post-shock region is obtained by enforcing post-shock equilibrium pressure at the outflow boundary condition. This model is referenced as "local steady-state shock tube". NASA Ames' electric arc shock tube (EAST) conditions are used. The results of both models are compared to a time-accurate simulation of the EAST shock tube [4].

This paper is structured as follows. In Sections II and III, we give a short description of the physical models and the related numerical methods. In section IV, we describe the computational setup for the full shock tube simulation and the proposed reduced problems. Herein, details of the computational domain, boundary conditions, and initial flow field are given. In Section V, we will discuss the results of the simulations. Finally, the conclusions are given in Section VI.

2 Physical models

Details of the physical models and numerical methods used in this work are given in [4], only a short description is provided here. The equations governing multi-component reactive flows are derived from the kinetic theory of polyatomic reactive gas mixtures [5, 6, 7]. These equations can be split between conservation equations, thermochemistry, and transport fluxes. The latter are computed based on the Chapman-Enskog [8, 9, 7] method. The thermodynamic properties of individual species are computed based on semi-classical statistical mechanics using quantized energy levels and Boltzmann statistics. The energy modes are considered decoupled, rotational and vibrational energies are computed according to the rigid rotor and harmonic oscillator models, respectively. The two-temperatures Park's model [10] is used. Vibrational-translational energy exchange is evaluated based on a Landau-Teller model [11], and the relaxation time is computed by the Millikan and White formula as proposed by Park [12].

3   Computational method

The system of coupled partial differential equations are discretized using the finite volume method [13]. The convective fluxes are computed using the $AUSM^+_{UP}$ scheme [14, 15, 16]. In order to get second order accuracy, each one of the cell centered state variables is linearly extrapolated to the face quadrature points. The linearly reconstructed state variables are calculated using a least-squares method [17]. In order to prevent the appearance of oscillations near discontinuities, a flux limiter is needed for the reconstructed states. In the present work, Venkatakrishnan's limiter [18] is used. The second order time accurate Crank-Nicolson scheme is used for time accurate simulation and forward Euler for steady cases. At each time step, the resulting linear system is solved implicitly using a Newton method. The latter requires a matrix inversion which is generally achieved by approximate methods. We use the Generalized Minimum RESidual (GMRES) algorithm, complemented with an Additive Schwartz pre-conditioner both provided by the PETSc library.

The CFD tool that is used in this simulation is COOLFluiD [19, 20] developed at the von Karman Institute, Belgium. COOLFluiD was subject to validation for many hypersonic flows at both steady and unsteady conditions. [21, 22, 23, 24, 25]. The thermochemistry and the transport properties are provided by the PLATO library which is developed at UIUC [26].

4   Numerical setup

Numerical simulations of the unsteady flow in the complete shock tube, steady flow around a cylinder, which is referenced in this work as the "stagnation-line" approach, and our "local steady state shock tube" are performed. Although the geometries are different, special care has been taken to ensure that the same grid spacing, $\Delta x = 10^{-3}m$, is applied. The starting case is unsteady flow inside a shock tube.

4.1   Unsteady flow inside a shock tube

Numerical simulation of the transient flow inside EAST facility has been performed using the total length of the eight meter tube. A two-dimensional uniform grid was used for this simulation, the level of refinement was chosen according to [27], with an axial spacing of $\Delta x = 10^{-3}m$. Only an inviscid simulation was ran, the viscous case was discussed in our previous work [4]. The configuration and boundary conditions are shown in Fig. 1.
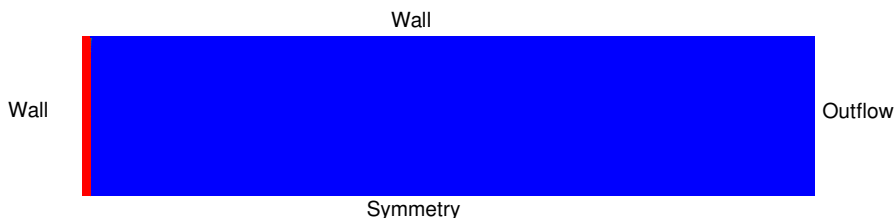

Figure 1: Schematic initial flow field showing the interface between the driver and the test gas

The supersonic boundary condition is imposed at the outflow, and a slip wall boundary condition is applied at the wall for the inviscid case. No-slip wall boundary conditions is

used in the viscous case. Air is used as the test gas -shown in blue in Fig. 1- , the driver gas is composed of 99% of Helium and 1% Nitrogen -shown in red in Fig. 1- . The initial conditions are the same for both viscous and inviscid cases and are given in Table 1.

	driver gas	test gas
	Y_{N_2} : 0.0144	Y_{N_2} : 0.79
	Y_{He}: 0.9856	Y_{O_2} : 0.21
ρ, kg/m^3	1.10546	3.0964 x 10^{-4}
T, K	6000	300
p, Pa	12.7116 x 10^6	26.771

Table 1: Initial conditions at diaphragm rupture

The results of the viscous and inviscid time accurate simulations, provide the predicted shock speed at the test section. This shock speed is used as an input for the flow over a cylinder, and the local steady-state shock tube problem. The shock speed has been calculated by considering the shock arrival at a certain location as a 10% pressure rise with respect to the undisturbed region i.e. the initial test gas pressure. Table 2 shows the difference of the shock speed between the viscous and the inviscid case and the corresponding equilibrium post-shock temperature, which was calculated using CEA[28].

Case	I: inviscid	II: viscous
Shock Speed, km/s	10.065	9.782
$T^{cea}_{equilibiurm}$, K	9992	9509

Table 2: Shock speed at test section

4.2 Stagnation Line approach

In this test-case, the stagnation line is obtained from a supersonic flow simulation over a 3m radius cylinder. The free steam conditions are the same as for the test gas - Tab. 2-. The free stream velocity is the shock speed, i.e 10.065 km/s and 9.782 km/s for the inviscid and viscous case, respectively. Fig. 2 shows the applied boundary conditions.
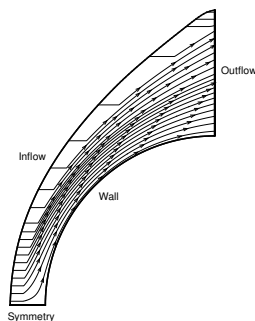

Figure 2: Stream lines showing flow over a 3 m cylinder, u_∞=9.782 km/s

The region of interest is the post-shock region along the stagnation line.

4.3 Local steady state shock tube

The computational domain in this test-case is a two-dimensional 0.3m long tube. Fig. 3 shows the domain with the boundary conditions. The post-shock condition region is shown in red. The inflow condition is supersonic and it is the same as the cylinder case, the outflow is subsonic, thus an adequate boundary condition needs to be applied. The equilibrium post-shock pressure is imposed at the outflow. It is obtained from CEA by considering the shock speed as inflow velocity.
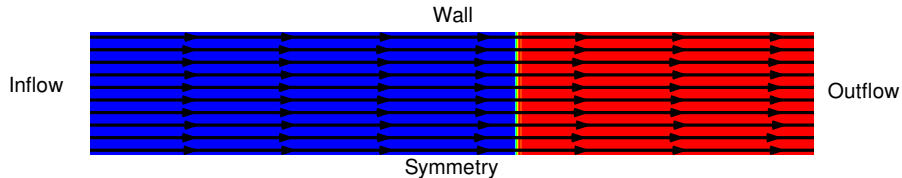

Figure 3: Computational domain and the stream lines, length of the domain is 0.3m

5 Results

The local steady-state shock tube problem result is compared to the stagnation-line approach and unsteady flow simulation of the complete shock tube. Both viscous and inviscid case are considered. Fig. 4(a) shows temperatures profiles of all three cases. They converge towards the same equilibrium value, that is T= 9992 K as predicted by CEA. The relaxation process for both the translational and vibrational temperature towards equilibrium is very similar between the stagnation-line approach and the local steady-state shock tube problem. It is, however, slightly different from the unsteady shock tube case, where the relaxation process is slower. This disagreement between the unsteady and steady cases is also noticeable on the number density profiles, shown in Fig. 4(b). The number density of $e-$ is larger in the steady case, and lower for N_2 and N_2^+.
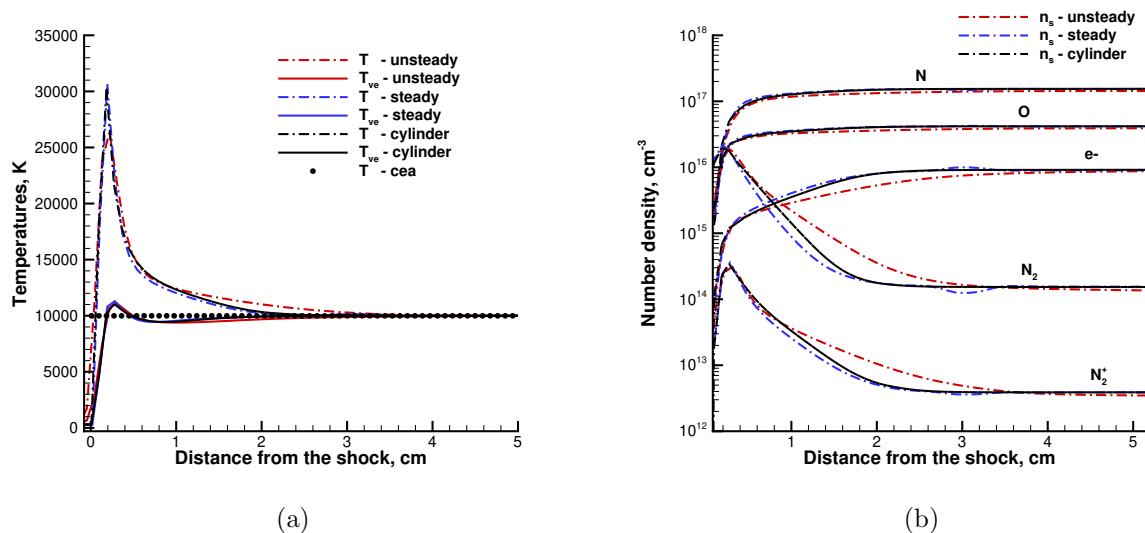

(a)

(b)

Figure 4: Post-shock temperature and number densitiy profiles, inviscid case -table. 2-

The reason for this discrepancy is believed to be related to the difference in the shock speed. In the steady case, the shock speed is imposed as a constant value, and it is the free stream velocity, applied at the inflow boundary conditions - see Figs. 2 and 3-. While for the unsteady case, the shock is traveling through the computational domain. Although, the shock speed is supposed to attain a constant value in the unsteady inviscid simulation; in our case it is never reached, and the shock is still slightly accelerating at the end of the shock tube. This numerical artifact is due to the strong dependence of shock speed on the grid size, which is $\Delta x = 10^{-3}$ m. This value is very coarse with regards to the magnitude of the gradients involved in the post-shock region, and thus introduces a numerical error when the shock jump from one cell to another. The choice of using this value was deliberately chosen in order to be consistent with the unsteady viscous simulations. The grid size of the latter was dictated by the quest to reduce the pharaonic computational cost.

The comparison with the unsteady viscous simulation, Fig. 5(a) and 5(b), shows a different trend. Because the shock is decelerating, the unsteady case reaches the post-shock equilibrium temperature, T=9509 K, around 1 cm after the shock location while for the steady case, the equilibrium is reached around 2.5 cm. Good agreement is obtained, again, between the cylinder and the local steady shock tube. This is not surprising, because only the boundary conditions values have changed, however it confirms the results seen with the inviscid conditions.
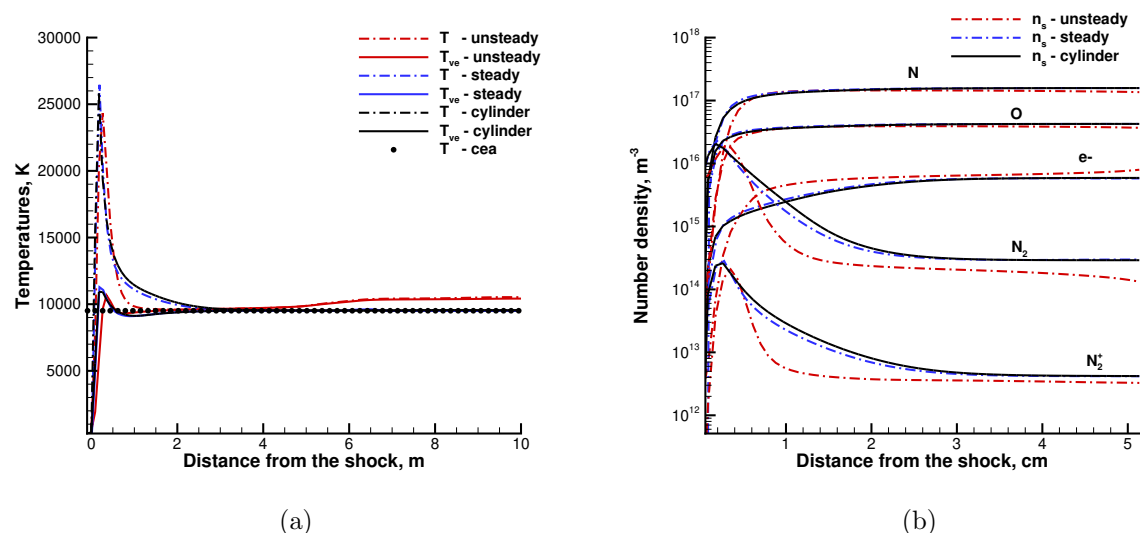

(a)   (b)

Figure 5: Post-shock temperature and number densitiy profiles, viscous case -table. 2-

The number of density profiles shown in Fig. 5(b) manifest the discrepancy between the steady and the viscous steady case. The number density of N_2 and N_2^+ species are higher in the steady case, and is lower for the electrons. An opposite trend has been found when comparing the steady and unsteady inviscid cases.

The impact of these differences between steady and the unsteady simulations on the radiative heat transfer is investigated through a non-equilibrium radiation calculation using an uncoupled approach. The flow solution, i.e temperatures and number densities for one line of sight, which is the symmetry boundary condition in all the cases, were passed to NEQAIR, with the radiance calculated. The non-Boltzmann population of the radiating state is considered. Figs 6(a) and 6(b) shows a comparison of the total radiance

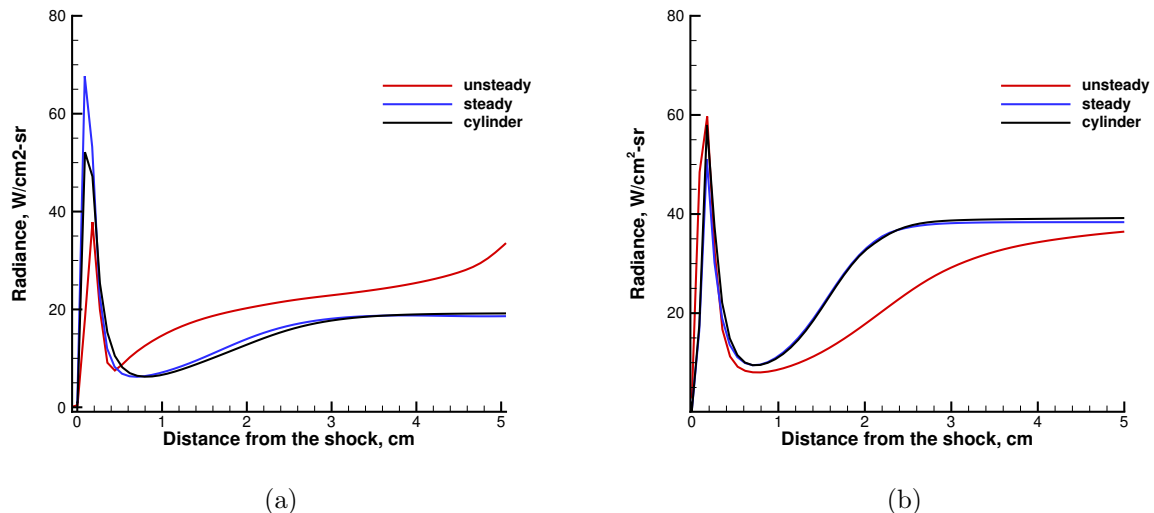for the viscous and inviscid conditions, respectively.

Figure 6: Radiance, a) viscous conditions, b) inviscid conditions

The stagnation-line approach and the local-steady shock tube problem compare fairly well. There is a significant difference in the total radiance between the steady approaches and the unsteady runs. Although, the differences in temperature profiles and the number densities did not seem significant, they do have a considerable impact on the total radiance. The unsteady shock speed effect may be the cause of these differences, additional investigations are on-going.

6 Conclusions

In this work, we explored different computational approaches for simulating non-equilibrium flows in shock tubes, with the main focus on duplicating shock layer radiation for planetary (re)-entry conditions. Both steady and unsteady cases were considered. The unsteady results were based on our previous work and were used as a reference case for the steady problems. The first steady case is a two-dimensional flow over a cylinder. This is the standard approach for calculating post-shock condition using the stagnation line, and it has been used with success over the last decade for validating the computational model with shock tube experiments. Nevertheless, the cylinder case presents several disadvantages: wall curvature effect, no boundary layer in the post-shock region, the shock layer radiation requires a higher grid resolution which increases drastically the number of degree of freedom. To overcome these pitfalls, a local steady-state shock tube approach was proposed. Good agreement was obtained between this approach and the cylinder for the translational and vibrational temperatures, number density profiles and total radiance. Both steady cases showed some disagreement with the unsteady simulation, which is attributed to shock speed unsteadiness. Unsteady runs with higher grid resolution are needed to affirm these observations. We believe that the local steady-state shock tube approach alleviates the drawbacks of the cylinder approach. It provides an accurate and efficient steady state alternative in simulating the experiment designed to reproduce shock layer radiation in shock tube facilities. It also opens a new door for a full coupling of the flow and the radiation solver, and more advanced kinetics such as state-to-state models.

References

[1] I. Nompelis. *Computational Study of Hypersonic Double-Cone Experiments for Code Validation.* PhD thesis, University of Minnesota, May 2004.

[2] Khalil Bensassi. *Contribution to the Numerical Modeling of the VKI Longshot Hypersonic Wind Tunnel.* ISBN 978-2-87516-072-0. von Karman Institute for Fluid Dynamics, 2014.

[3] Richard J. Goozee. *Simulation of a Complete Shock Tunnel Using Parallel Computer Codes.* PhD thesis, Division of Mechanical Engineering, University of Queensland, 2003.

[4] Khalil Bensassi and Aaron M. Brandis. Time accurate simulation of nonequilibrium flow inside the nasa ames electric arc shock tube. In *AIAA Scitech 2019 Forum*, number AIAA 2019-0798.

[5] J. O. Hirschfelder, C. F. Curtiss, and R. B. Bird. *Molecular theory of gases and liquids.* John Wiley and Sons, New York, 1967.

[6] Ekaterina Nagnibeda and Elena Kustova. *Non-Equilibrium Reacting Gas Flows: Kinetic Theory of Transport and Relaxation Processes.* Heat and Mass Transfer. Springer Berlin Heidelberg, 2009.

[7] V. Giovangigli. *Multicomponent flow modeling.* Birkhäuser, 1999.

[8] S. Chapman and T.G. Cowling. *The Mathematical Theory of Non-Uniform Gases.* Cambridge University Press, London, U.K., 1970.

[9] J. H. Ferziger and H. G. Kaper. *Mathematical theory of transport processes in gases.* North-Holland Publishing Company, Amsterdam–London, 1972.

[10] C. Park. *Nonequilibrium Hypersonic Aerothermodynamics.* John Wiley and Sons, New York, 1989.

[11] L. Landau and E. Teller. Theory of sound dispertion. *Physikalische Zeitschrift der Sowjetunion*, 10(34), 1936.

[12] Chul Park. Review of chemical-kinetic problems of future nasa missions. i - earth entries. *Journal of Thermophysics and Heat Transfer*, 7(3):385–398, 1993.

[13] Timothy Barth and Mario Ohlberger. Finite volume methods: Foundation and analysis. In Ltd John Wiley & Sons, editor, *Encyclopedia of Computational Mechanics*, 2004.

[14] M. S. Liou and C. J. Jr. Steffen. A new flux splitting scheme. *Journal of Computational Physics*, 107:23–39, 1993.

[15] M. S. Liou. A sequel to ausm: Ausm+. *Journal of Computational Physics*, 129:363–382, 1996.

[16] M. S. Liou. A further development of the ausm$^+$ scheme towards robust and accurate solutions for all speeds. In *16th AIAA Computational Fluid Dynamics Conference*, Orlando, Florida, June 2003. AIAA 2003-4116.

[17] Timothy Barth. Aspects of unstructured grids and finite volume solvers for the euler and navier-stokes equations. 25th Computational Fluid Dynamics Lecture Series. Von Karman Institute, March 1994.

[18] S. Venkateswaran and Ch. L. Merkle. Analysis of preconditioning methods for the Euler and Navier-Stokes equations. VKI LS 1999-03, von Karman Institute for Fluid Dynamics, St.-Genesius-Rode, Belgium, March 1999.

[19] Andrea Lani, Tiago Quintino, Dries Kimpe, and Herman Deconinck. The coolfluid framework - design solutions for high-performance object oriented scientific computing software. In *International Conference Computational Science 2005*, volume 1, pages 281–286, Atlanta, 2005. Springer-Verlag.

[20] A. Lani, T. Quintino, D. Kimpe, H. Deconinck, S. Vandewalle, and S. Poedts. The COOLFluiD framework: Design solutions for high-performance object oriented scientific computing software. In P. M. A. Sloot V. S. Sunderan, G. D. van Albada and J. J. Dongarra, editors, *Computational Science ICCS 2005*, volume 1 of *LNCS 3514*, pages 281–286, Atlanta, GA, USA, May 2005. Emory University, Springer.

[21] M. Panesi, A. Lani, T. Magin, F. Pinna, O. Chazot, and H. Deconinck. Numerical investigation of the non equilibrium shock-layer around the expert vehicle. In *AIAA Paper 2007-4317*, Miami (Florida), Jun 2007. 38th AIAA Plasmadynamics and Lasers Conference.

[22] Khalil Bensassi, Andrea Lani, Patrick Rambaud, and O. Chazot. Numerical simulation of hypersonic flow in vki-longshot contoured nozzle. In *40th Fluid Dynamics Conference and Exhibit*, number AIAA-2010-4857. American Institute of Aeronautics and Astronautics, 2010.

[23] Khalil Bensassi, Andrea Lani, and Patrick Rambaud. Numerical investigations of local correlation-based transition model in hypersonic flows. In *42nd AIAA Fluid Dynamics Conference and Exhibit*, number AIAA-2012-3151. American Institute of Aeronautics and Astronautics.

[24] Khalil Bensassi, Andrea Lani, Olivier Chazot, and Patrick Rambaud. Arbitrary lagrangian eulerian simulation of a moving piston in hypersonic ground test facility. In *42nd AIAA Fluid Dynamics Conference and Exhibit*, number AIAA-2012-3265. American Institute of Aeronautics and Astronautics, 2012.

[25] K. Bensassi, A. Lani, and P. Rambaud. Unsteady simulation of hypersonic flow around a heat flux probe in ground testing conditions. *International Journal of Heat and Mass Transfer*, 113:889 – 897, 2017.

[26] Alessandro Munafo. Plasmas in thermodynamic non-equilibrium (plato) library, munafo@illinois.edu.

[27] Dmitry V. Kotov, H.C. Yee, Marco Panesi, Dinesh K. Prabhu, and Alan A. Wray. Computational challenges for simulations related to the nasa electric arc shock tube (east) experiments. *Journal of Computational Physics*, 269(Supplement C):215 – 233, 2014.

[28] Christopher A. Snyder. Chemical equilibrium with applications, https://www.grc.nasa.gov/www/ceaweb/.